ELSEVIER

Int. J. Pres. Ves. & Piping 60 (1994) 71–83

0308-0161/94/$07.00

A database to evaluate stress intensity factors of elbows with throughwall flaws under combined internal pressure and bending moment

J. Chattopadhyay, B. K. Dutta,* H. S. Kushwaha, S. C. Mahajan & A. Kakodkar

Reactor Design and Development Group, Bhabha Atomic Research Centre, Trombay, Bombay-400085, India

(Received 10 August 1993; accepted 24 September 1993)

The advent of the leak-before-break (LBB) concept has widely replaced the traditional design basis event of a double-ended guillotine break (DEGB) in the design of primary heat transport (PHT) piping. The use of the LBB concept requires postulation of the largest credible cracks at highly stressed locations and demonstration of their stability under the maximum credible loading conditions. Stress analysis of PHT piping in nuclear power plants shows that the highly stressed piping components are normally elbows and branch tees. This necessitates detailed fracture mechanics evaluation of such piping connections by computing their stress intensity factors (SIF) and/or J-integral. Simple analytical solutions for evaluation of the SIF and J-integral for cracks in straight pipes are readily available in the literature. However the same type of solution for elbows and tees is limited in the open literature. In the present work a database is generated to evaluate the SIF for throughwall circumferential and longitudinal cracks under combined internal pressure and bending moment. Different parameters used to characterise a cracked elbow are pipe factor (h), pipe bore radius to thickness ratio (r/t) and crack length. Another parameter (ρ) is used to consider the relative magnitude of stresses due to internal pressure and remote bending moment. This database has been used to derive closed-form expressions to evaluate the SIF for elbows with cracks in terms of the aforementioned parameters.

NOTATION

a	Semi-crack length
A	Area enclosed by the integration path Γ
A_e	$= K_{\text{mid}}/\sigma_r\sqrt{\pi a}$, a non-dimensional parameter to define SIF.
E	Young's modulus
h	$= tR/r^2$, pipe factor
J_k	J-integral in local x,y and z directions ($k = x, y, z$)
K	Stress intensity factor (SIF)
K_i	SIF computed at radial distance r_i
K_{mid}	SIF at mid-layer
M	Remote bending moment
n	Number of sampling points considered to evaluate $(\text{SIF})_c$
n'_k	Normal to the evaluation layer
n_k	Normal to the integration path Γ
P	Internal pressure
r	Mean pipe radius
r_i	Radial distance of the sampling point from crack tip to evaluate $(\text{SIF})_c$
R	Mean pipe bend radius
$(\text{SIF})_c$	SIF extrapolated to the crack tip
t	Pipe thickness
u_i	Displacements
W	Strain energy density
Γ	Integration path to evaluate J-integral
θ	Angle subtended by the elbow axis at the bend centre
θ_c	Angle subtended by the longitudinal semi-crack on elbow at the bend centre
λ	$= a\sqrt{rt}$, longitudinal crack length in non-dimensional form

* To whom correspondence should be addressed.

λ_c $[12(1-\nu^2)^{0.25} . a/\sqrt{rt}$, shell parameter to define crack length in cylinder
ν Poisson's ratio
ρ $= (2/\pi) . (M/pr^3)$, load ratio to define relative magnitude of internal pressure and bending moment
σ_{ij} Stress tensor along the integration path Γ
σ_r Reference stress in defining A_e
ϕ Angle subtended by the elbow circumference at cross-sectional centre at a particular θ
ϕ_c Semi-circumferential crack angle on an elbow

1 INTRODUCTION

The safety of nuclear reactors has always engaged the attention of the designers of such plants. The piping system which enables cooling of the reactor core has been one of the important items where considerable research has been carried out. A failure in the piping could lead to a loss-of-coolant accident and may lead to the release of radioactive materials to the public domain. Hence one of the current active research areas is the fracture mechanics evaluation of piping components with the presence of flaws.

One of the hypothetical design basis events traditionally considered in the design of primary heat transport (PHT) piping of a pressurised heavy water reactor (PHWR) is an instantaneous double-ended guillotine break (DEGB) of the largest heat transport pipe. This concept was originally initiated for sizing the containment and emergency core cooling systems (ECCS). Regulatory philosophy for the design of piping systems, however, tended to shift the postulate of DEGB to a design basis for making provisions of protection against DEGB. A natural consequence of an accepted pipe break postulate would require provision of massive pipe whip restraints to minimise pipe deflection.

However, over the years it has been found that these restraints have resulted in many problems such as: restricted access for in-service inspection and hence additional expenditure; complication in pipe system design; increased heat loss to the surrounding environment; and unanticipated thermal expansion stress. Against this backdrop, the nuclear community has started giving second thoughts to the real efficacy of the pipe rupture protection devices in enhancing the safety of the plant. The question being asked is whether these devices really increase plant safety or not. With this background, the United States Nuclear Regulatory Commission (USNRC) formed a pipe break task group to investigate the probability of an occurrence of catastrophic pipe rupture. The task group findings show that there is vanishingly low probability of pipe rupture under all circumstances[1] provided one adopts well directed design and in-service maintenance procedures. Consequently, USNRC recommended the elimination of the requirements of mechanical pipe rupture protection against the arbitrary intermediate breaks and henceforth the replacement of the traditional design basis event of DEGB by the concept of leak-before-break (LBB) in the design of a piping system. The LBB approach means the application of fracture mechanics technology to demonstrate that the piping is very unlikely to experience double-ended rupture or its equivalent as longitudinal or diagonal splits. The methodology consists of demonstrating three levels of confidence. These three levels of confidence may be viewed as a defence in depth strategy. Level 1 confidence is inherent in the design philosophy of ASME Section III which is normally followed in piping design. The design is done with a well defined factor of safety. However, it does not consider the presence of any flaw in the pipe. Level 2 consists of postulating a part-through crack at the inside surface of the PHT piping and then demonstrating that it will not grow throughwall during the period between two successive in-service inspections/repairs or, possibly, during the entire life period of the reactor. It should be also shown that the final flaw size at the end of the evaluation period is sufficiently smaller than the critical flaw. Level 3 postulates a throughwall crack that will ensure detectable leakage and then demonstrates that the crack will be stable under the maximum credible loading conditions.

2 SCOPE OF THE PRESENT WORK

The LBB approach requires the extensive application of fracture mechanics for the piping system with the presence of a flaw. It postulates the largest credible flaw at the highly stressed points in the piping system and demonstrates its stability under the most severe loading condi-

tions. Stress analysis of PHT piping in a nuclear power plant shows that highly stressed piping components are normally elbows and tees. This necessitates detailed fracture mechanics evaluation of piping components by computing the stress intensity factor (SIF) and/or the J-integral. Simple analytical solutions for the SIF and J-integral are available for straight pipes.[2,3] However, the same type of solutions is not available for elbows and tees in the open literature. Hence, a computational technique (e.g. the finite element method) is adopted to evaluate the solutions for elbows and tees. However, the application of the finite element method requires a high level of expertise and large computation times. In the present work, a database is generated to evaluate the SIF for various sizes of elbows with various sizes of flaws under different types of loadings. The authors have also tried to derive closed-form expressions by using this database to evaluate stress intensity factors for throughwall flaws in elbows as a function of different geometrical parameters and loadings.

3 DEVELOPMENT OF A FINITE ELEMENT CODE 'FABS'

To carry out the above-mentioned task of analysing elbows with throughwall flaws, a finite element code 'FABS' (fracture mechanics analysis of bending structure) has been developed. It uses nine-noded heterosis/eight-noded degenerate shell bending elements. Stresses along the thickness are considered using a layered approach. Each layer contains stress points and the stresses are assumed to be constant over the thickness of each layer. Thus, the actual stress distribution is modelled by a piecewise constant approximation. The capability of the code has further been enhanced by adding subroutines to calculate the J-integral using a contour approach at different layers of thickness in a three-dimensional body. The database of the SIF has been generated using this code. Considering the large number of case studies needed to be done to generate the database, a versatile pre-processor has been developed which generates element topology, nodal coordinates, boundary conditions and loading data. The output of this pre-processor is compatible with the input data of the code 'FABS'. The output of the code 'FABS' is then further processed to get the SIF expressed in a non-dimensional form, A_e, where A_e is expressed as:

$$A_e = K_{mid}/\sigma_r\sqrt{\pi a} \tag{1}$$

4 EVALUATION OF THE STRESS INTENSITY FACTOR

There are a number of methods to evaluate the SIF. However, only two, namely the displacement correlation and J-integral methods, have been adopted here.

In case of the displacement correlation method, the SIFs have been evaluated by considering the crack face nodes only. However the normal procedure for evaluating the SIF by extrapolating a straight line on graph paper can be more of an art where uniqueness is lost.[4] Hence in the present work, a best fit straight line equation is used for a number of nodes and then extrapolated to the crack tip to get a unique solution of the SIF. The equation used for this extrapolation is:

$$(\mathrm{SIF})_c = \sum (K_i - \beta r_i)/n \tag{2}$$

where:

$$\beta = [n\sum K_i r_i - \sum K_i \sum r_i]/[n \sum r_i^2 - (\sum r_i)^2] \tag{3}$$

As mentioned above, the authors have also implemented the J-integral procedure to evaluate the SIFs. The expression which has been used in the present study for J-integral evaluation is given below:[5]

$$J_k = \int_\Gamma (Wn_k - \sigma_{ij} \,.\, n_j[\partial u_i/\partial k])\, \mathrm{d}\Gamma + \int_A \{n_k \,.\, \partial W/\partial z' - \partial(\sigma_{ij} \,.\, n_j' \,\partial u_i/\partial k)/\partial z\}\, \mathrm{d}A \tag{4}$$

5 ANALYSIS OF STRAIGHT PIPES WITH CRACKS

A number of case studies have been done to test the different capabilities of the present code to compute the stress intensity factor and J-integral

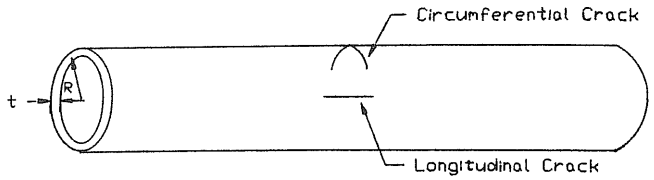

Fig. 1. A straight pipe with longitudinal and circumferential cracks.

of the structures containing flaws. These are described in Ref. 6. The details of the analyses done to compute the SIF for straight pipes with circumferential and longitudinal cracks under internal pressure are given below.

Figure 1 shows the details of circumferential and longitudinal cracks on a straight pipe. The pipe is subjected to internal pressure. A parametric study is carried out to evaluate the SIF expressed in terms of A_e for different r/t and crack length. Crack length is expressed in terms of a shell parameter (λ_c) which is expressed as:

$$\lambda_c = [12(1-\nu^2)]^{0.25} \cdot a/\sqrt{(rt)} \qquad (5)$$

The authors have computed the SIFs without considering the crack face loading. A separate case has also been analysed by considering the crack face loading being equal to internal pressure. To calculate A_e from eqn (1) the reference stress σ_r is taken as nominal hoop stress (pr/t) in the case of a longitudinal flaw and nominal axial stress ($pr/2t$) in the case of a circumferential flaw.

Figures 2 and 3 show the variation of A_e with shell parameter for a circumferentially cracked pipe. Figures 4 and 5 show the similar results for a longitudinally cracked pipe. The figures also compare these results with those quoted in Ref. 7.

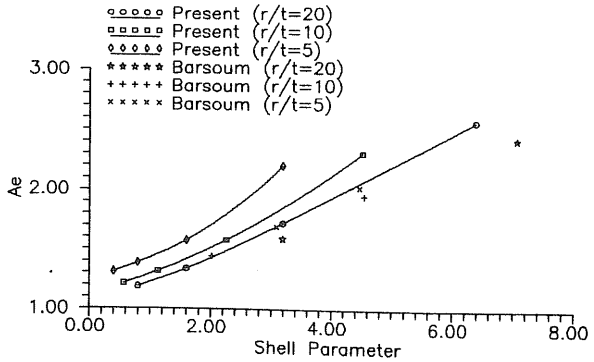

Fig. 2. Variation of A_e with shell parameter for a circumferentially cracked straight pipe (with crack face loading).

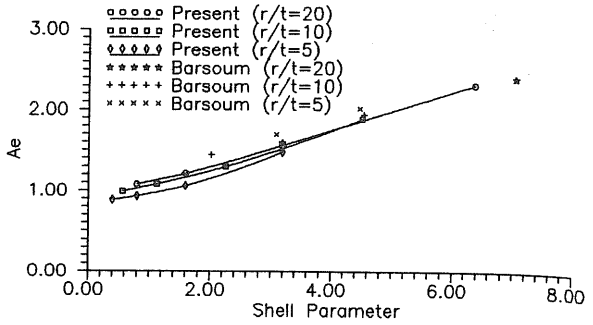

Fig. 3. Variation of A_e with shell parameter for a circumferentially cracked straight pipe (no crack face loading).

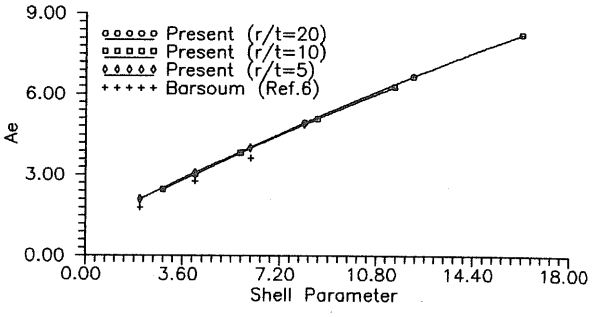

Fig. 4. Variation of A_e with shell parameter for a longitudinally cracked straight pipe (with crack face loading).

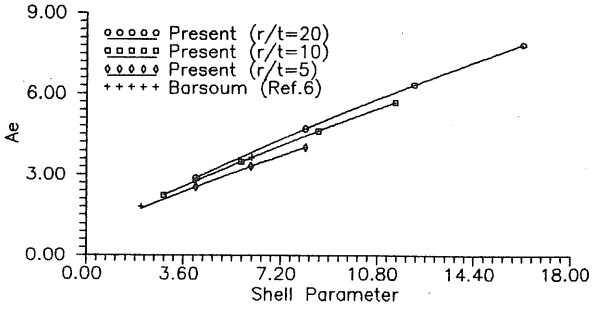

Fig. 5. Variation of A_e with shell parameter for a longitudinally cracked straight pipe (no crack face loading).

6 FINITE ELEMENT ANALYSIS OF A NON-WEAKENED ELBOW AND COMPARISON OF RESULTS WITH ANALYTICAL VALUES

Prior to analysing an elbow with a crack, a non-weakened elbow has been analysed to compute the stresses by the present computer code and the results have been compared with the analytical values. This exercise is done to test the capability of the present element in modelling an elbow under various types of loadings. Figure 6 shows the geometry of an elbow. Figure 7

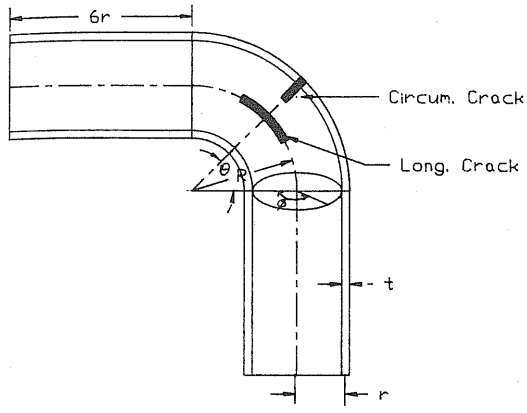

Fig. 6. Geometric details of an elbow and locations of various postulated cracks.

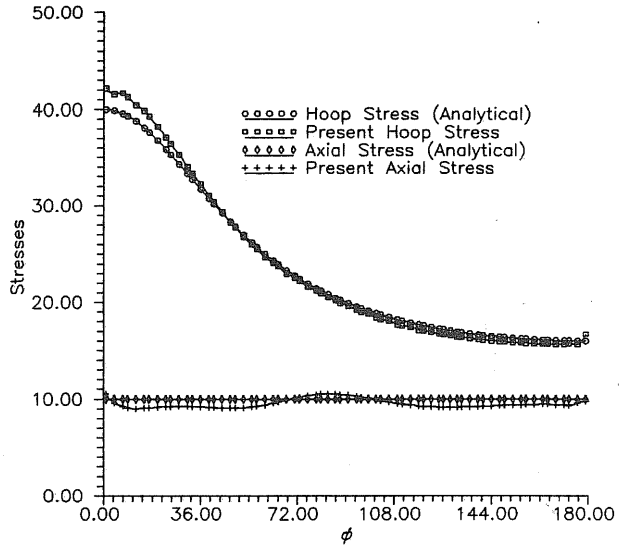

Fig. 7. Hoop and axial stress variation on the mid-plane of an elbow under internal pressure ($h = 0{\cdot}075$, $r/t = 20$).

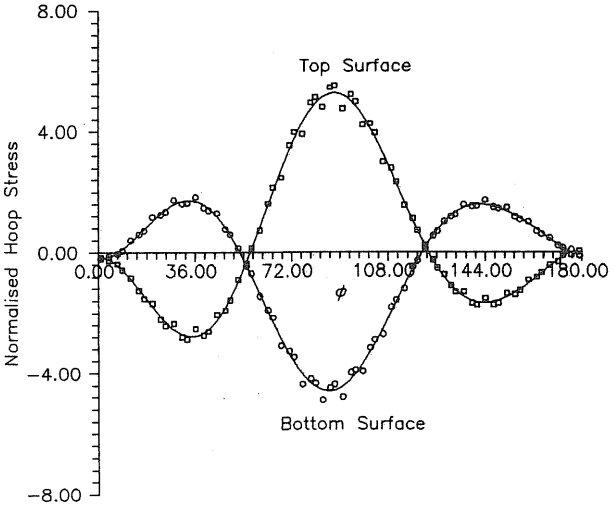

Fig. 8. Hoop stress variation on the mid-plane of an elbow under remote bending moment ($h = 0{\cdot}25$).

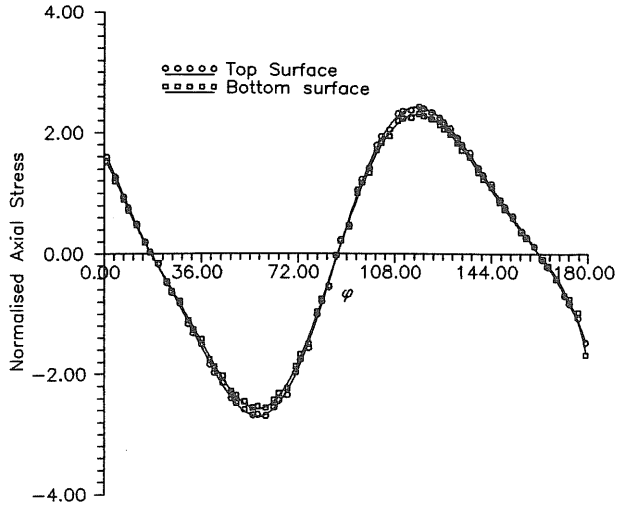

Fig. 9. Axial stress variation on the mid-plane of an elbow under remote bending moment ($h = 0{\cdot}25$).

shows the computed stresses for an elbow under internal pressure on the $\theta = 45°$ plane. The same figure also shows the analytical values.[8] The variation shows that longitudinal stress is constant along the circumference and hoop stress varies from its maximum at the intrados to the minimum at the extrados. Figures 8 and 9 show the variation of computed hoop and longitudinal stresses for the elbow subjected to remote bending moment. The stress distribution shows that the maximum hoop stress ocurs at $\phi = 90°$. Hence in the subsequent analysis the longitudinal crack has been postulated at $\phi = 90°$ with its centre on the $\theta = 45°$ plane and the circumferential crack has been postulated on the $\theta = 45°$ plane with its centre at $\phi = 180°$.

7 PARAMETRIC STUDY OF AN ELBOW WITH A CIRCUMFERENTIAL CRACK

A detailed parametric study of elbows with circumferential throughwall cracks under combined loading of closing bending moment and internal pressure has been carried out. Figure 6 shows the location of a circumferential crack on the elbow. The elbow has been modelled along with the connecting straight pipe. The length of the straight pipe is chosen as six times the radius of the pipe to eliminate the boundary effect. Only one fourth of the elbow is modelled due to symmetry. The finite element model consists of 552 eight-noded thick shell bending elements and

Table 1. Different combinations of r/t and pipe factor

r/t	Different pipe factors considered					
20	0·075	0·15	0·25	0·35	0·50	0·65
10		0·15	0·25	0·35	0·50	0·65
5				0·35	0·50	0·65

1751 nodes. The crack tip singularity is modelled by using quarter-point crack tip elements. The structure is assumed to be in the elastic condition. Three parameters are chosen to characterise an elbow with a circumferential crack, namely r/t, ϕ_c and pipe factor (h). Another parameter is chosen to consider the relative magnitude of stresses due to internal pressure and bending moment. It is expressed as:

$$\rho = (2/\pi) \,.\, (M/pr^3)$$

$\rho = 0$ indicates internal pressure only and $\rho = \infty$ indicates bending moment only.

The parametric study involves the evaluation of the SIF for different pipe factors, crack angles, r/t and load ratios (ρ). Table 1 shows the various combinations of r/t and pipe factors considered for the present analysis. The range of h considered is different for various r/t ratios, because the minimum possible value of h is restricted by t/r. The maximum value of the pipe factor is decided by considering the application of the database to primary heat transport piping. A typical h value for PHWR PHT piping is 0·5. Hence, the maximum value of h is restricted to 0·65. For each pipe factor, computations are done, for six different crack angles ($2\phi_c = 50°$, 90°, 120°, 140°, 160° and 180°) and for five different load ratios ($\rho = \infty$, 2, 1, 0·5 and 0). It has been seen that pure closing bending moment cannot open a small circumferential crack at the extrados. Hence, a small crack angle has not been included in the present parametric study.

In this manner a database has been generated by calculating A_e for various crack angles ($2\phi_c$), pipe factors (h), r/t and load ratios (ρ). There are 404 different cases in this database. The A_e is calculated by using eqn (1) for each case. The reference stress (σ_r) is taken as:

$$\sigma_r = (pr/2t) + (M/\pi r^2 t) \qquad (6)$$

For each case, A_e is calculated by computing the SIF using two independent methods. These are the displacement correlation method and the J-integral method. Figures 10a–10c show the variation of A_e with pipe factor (h), crack angle ($2\phi_c$) and r/t for different load ratios (ρ).

8 PARAMETRIC STUDY OF AN ELBOW WITH LONGITUDINAL CRACK

A parametric study of elbows with longitudinal crack has also been carried out along similar lines as explained above. Figure 6 shows the location of the longitudinal crack at $\phi = 90°$ of an elbow. Only half of the elbow is modelled due to symmetry. There are 484 eight-noded thick shell elements and 1484 nodes. The parameters chosen to characterise the elbow and loading are the same as before except that the crack length is expressed as:

$$\lambda = a/\sqrt{(rt)}$$

In the present case, five different values of λ ($\lambda = 0·5$, 1·0, 1·5, 2·0 and 2·5) and four different values of load ratio ($\rho = 2·0$, 1·0, 0·5 and 0·0) have been considered. $\rho = \infty$ could not be considered in the present case as a pure closing bending moment (where internal pressure is equal to zero) cannot open a longitudinal crack fully.

Here also, a database is generated for the SIF expressed in terms of A_e for different parameters as mentioned above. Figure 11 shows a typical deformed plot of a longitudinally cracked elbow under internal pressure. Figures 12a and 12b show the variation of A_e with pipe factors, crack length and r/t for different load ratios.

9 CLOSED-FORM EXPRESSIONS OF THE SIF FOR A CRACKED ELBOW

A closed-form expression is being proposed here to evaluate the stress intensity factor of an elbow with longitudinal and circumferential cracks under the combined loading of internal pressure and remote bending moment. The SIF is expressed in terms of a non-dimensional number (A_e) as defined in eqn (1). A reference stress (σ_r) is taken as defined in eqn (6). The A_e is expressed as a function of pipe factor (h), r/t and λ or θ_c/π (depending on whether the crack is longitudinal or circumferential). In the case of a longitudinal crack, the general expression used

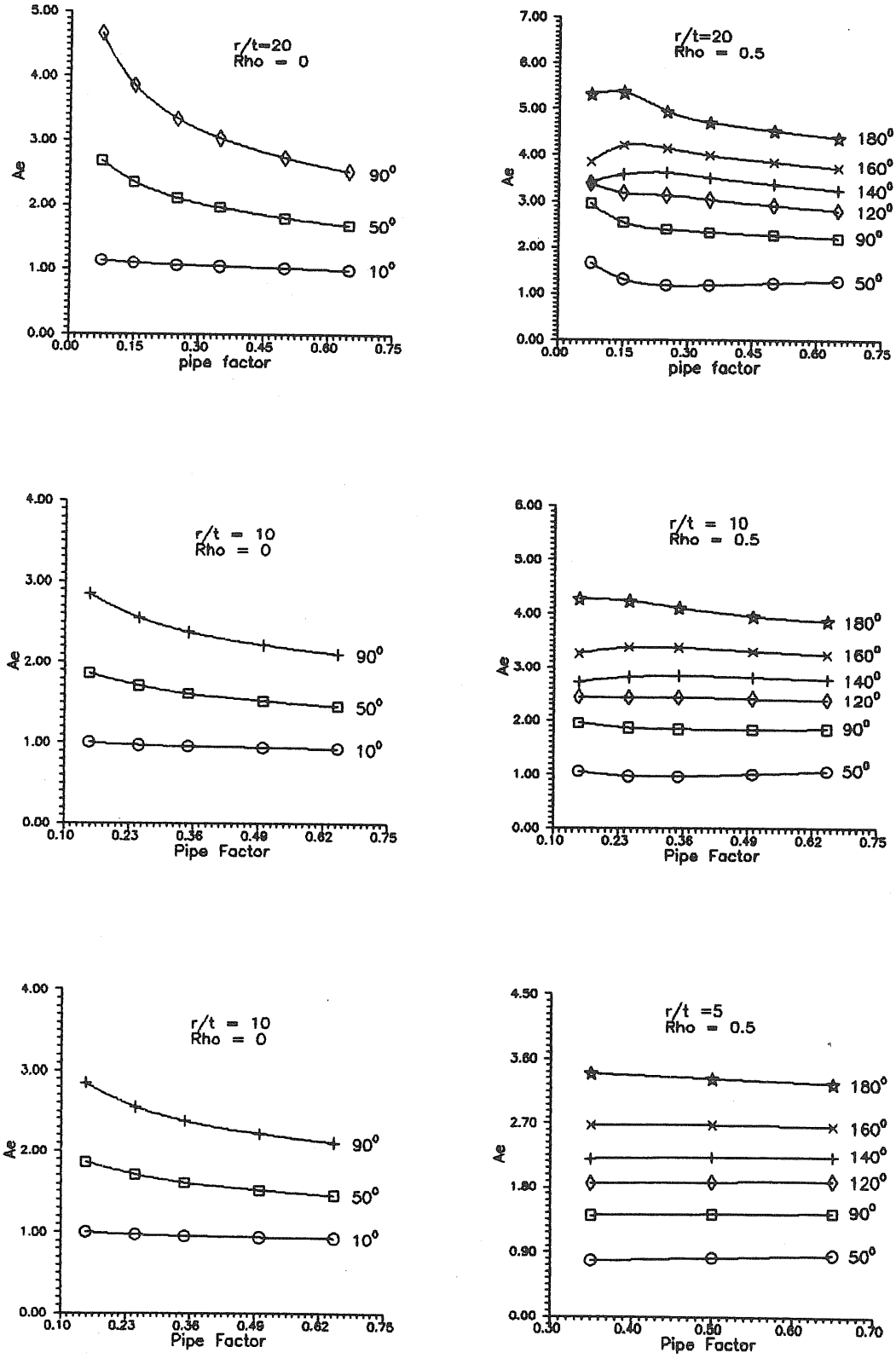

Fig. 10a. Variation of A_e with pipe factor (h), r/t and crack angle ($2\phi_c$) for a circumferentially cracked elbow ($\rho = 0,\ 0{\cdot}5$).

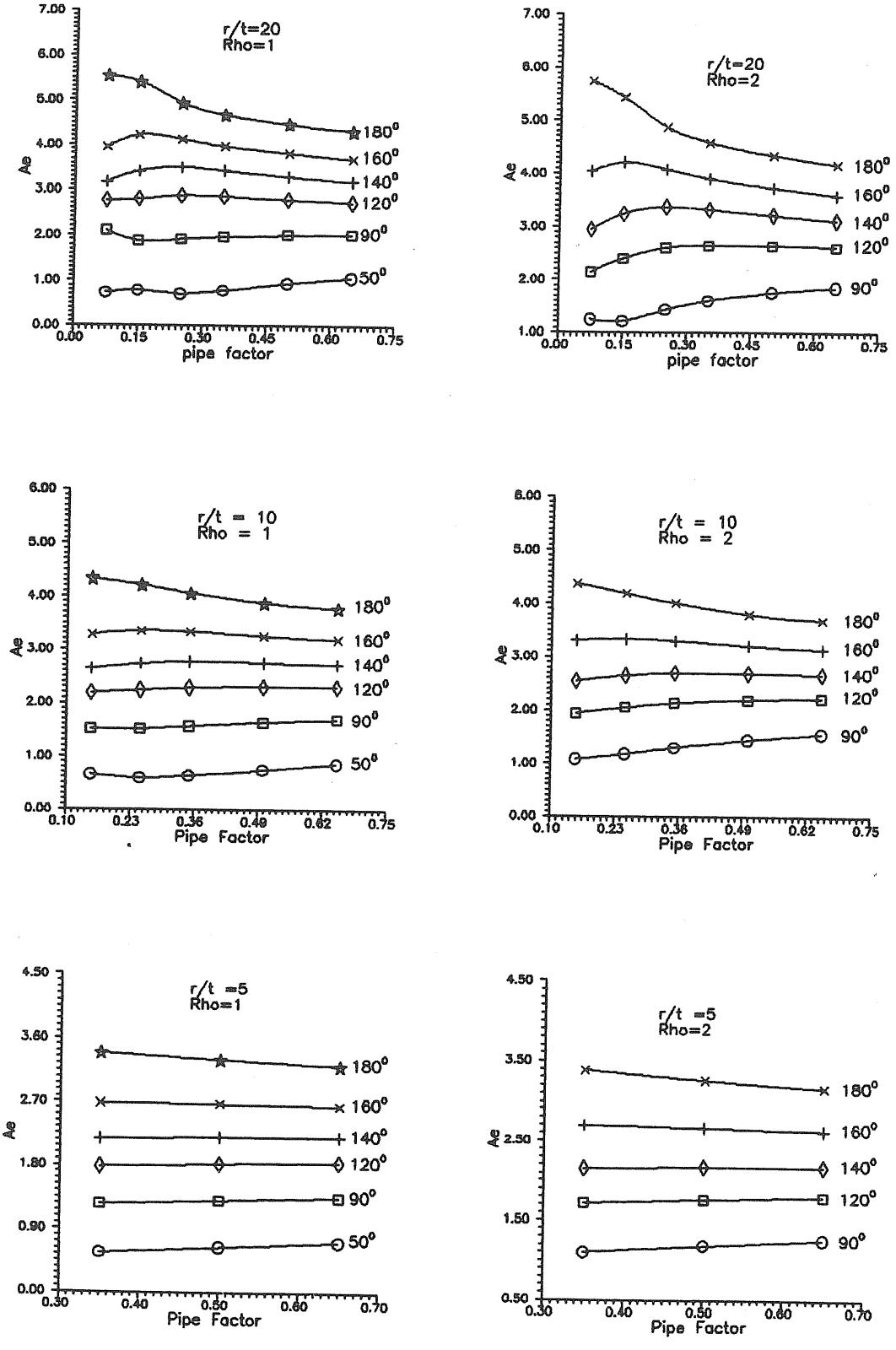

Fig. 10b. Variation of A_e with pipe factor (h), r/t and crack angle ($2\phi_c$) for a circumferentially cracked elbow ($\rho = 1, 2$).

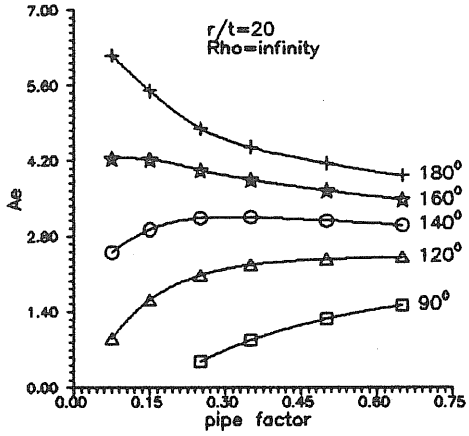

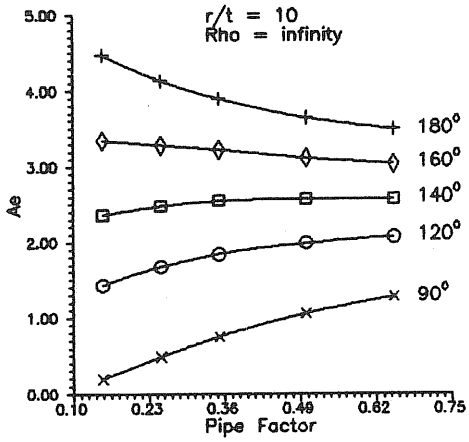

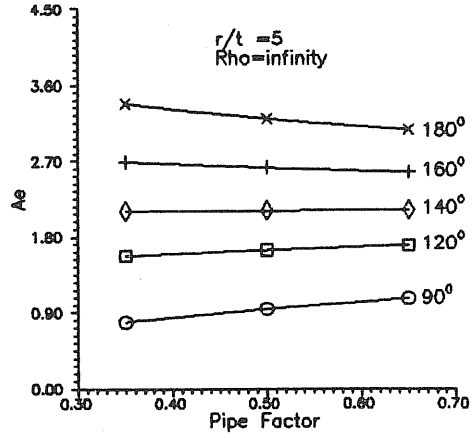

Fig. 10c. Variation of A_c with pipe factor (h), r/t and crack angle ($2\phi_c$) for a circumferentially cracked elbow ($\rho = \infty$).

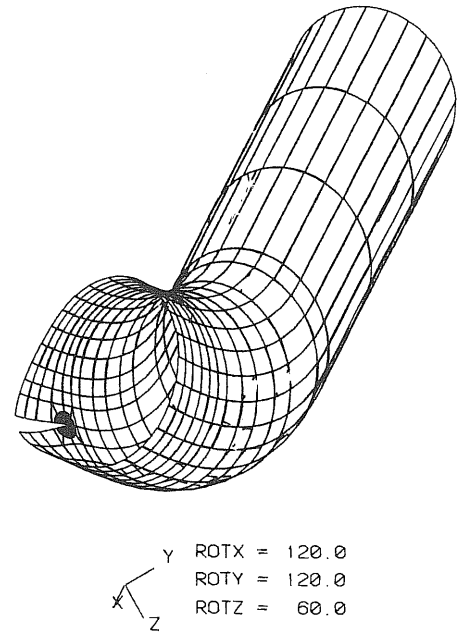

Fig. 11. Deformed plot of a longitudinally cracked elbow under internal pressure. Magnification factor of deformation = 10·00.

for A_c is:

$$A_c = (C_1 + C_2 h^{p_1}) + (C_3 + C_4 h^{p_2}) \cdot \lambda^{p_3} + [(C_5 + C_6 h^{p_4}) + (C_7 + C_8 h^{p_5}) \cdot \lambda^{p_6}] \cdot (t/r)^{p_7} \quad (7)$$

λ in the above expression is substituted by θ_c/π for a circumferential crack. The coefficients (C_n) and exponents (p_n) are evaluated by the least squares curve fitting method. Tables 2 and 3 show the values of C_n and p_n for different load ratios (ρ) for circumferential and longitudinal cracks, respectively.

10 CONCLUSIONS

(a) A finite element code 'FABS' has been developed for fracture mechanics analysis of structures containing defects using degenerate shell bending elements. The code has been validated against a number of sample problems which are described in Ref. 6.

(b) The code has been used to analyse straight pipes with cracks under internal pressure. Two cases have been considered. One of the cases accounts for crack face loading equal to internal pressure and another does not consider crack face loading. The results quoted in Ref. 7 lie

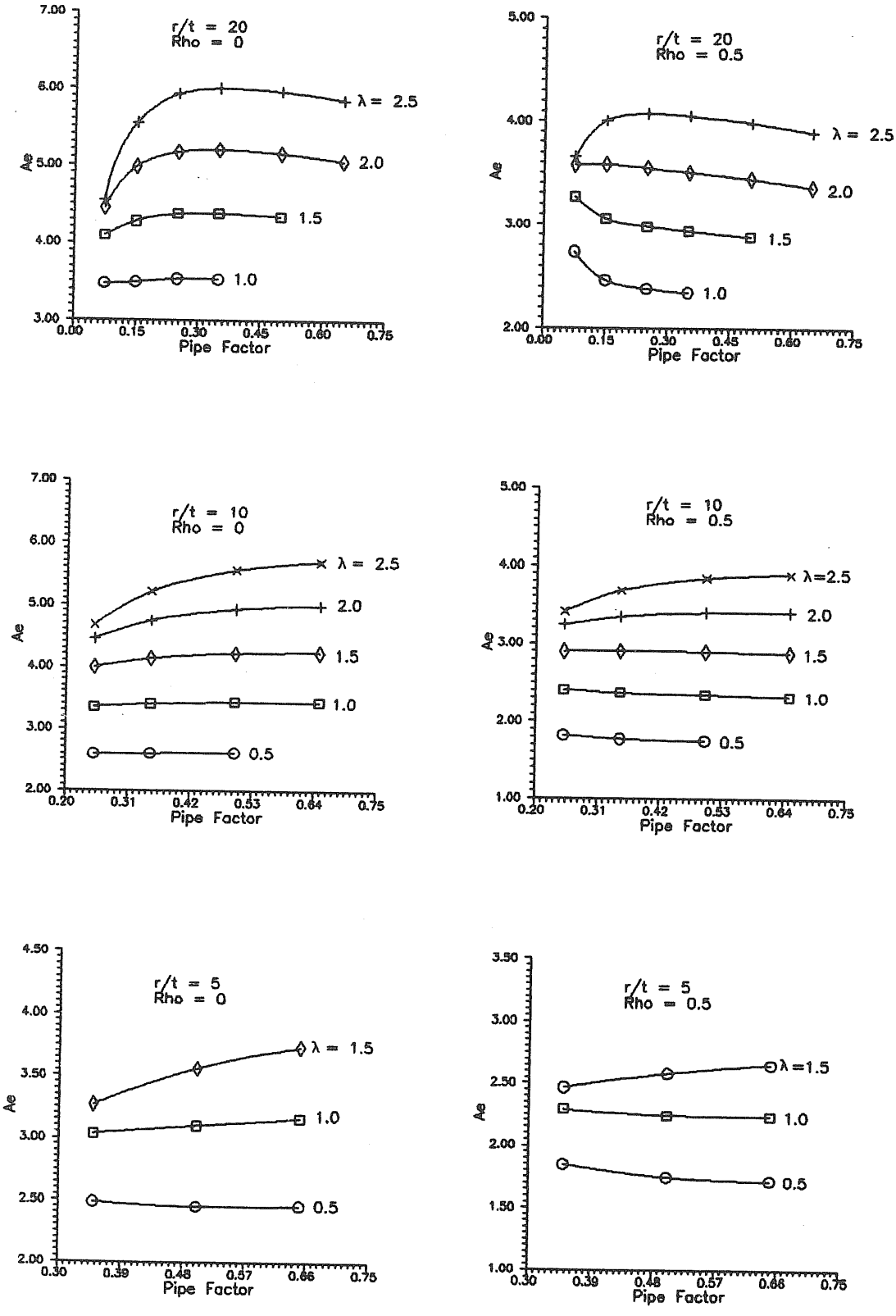

Fig. 12a. Variation of A_e with pipe factor (h), r/t and crack length (λ) for a longitudinally cracked elbow ($\rho = 0, 0{\cdot}5$).

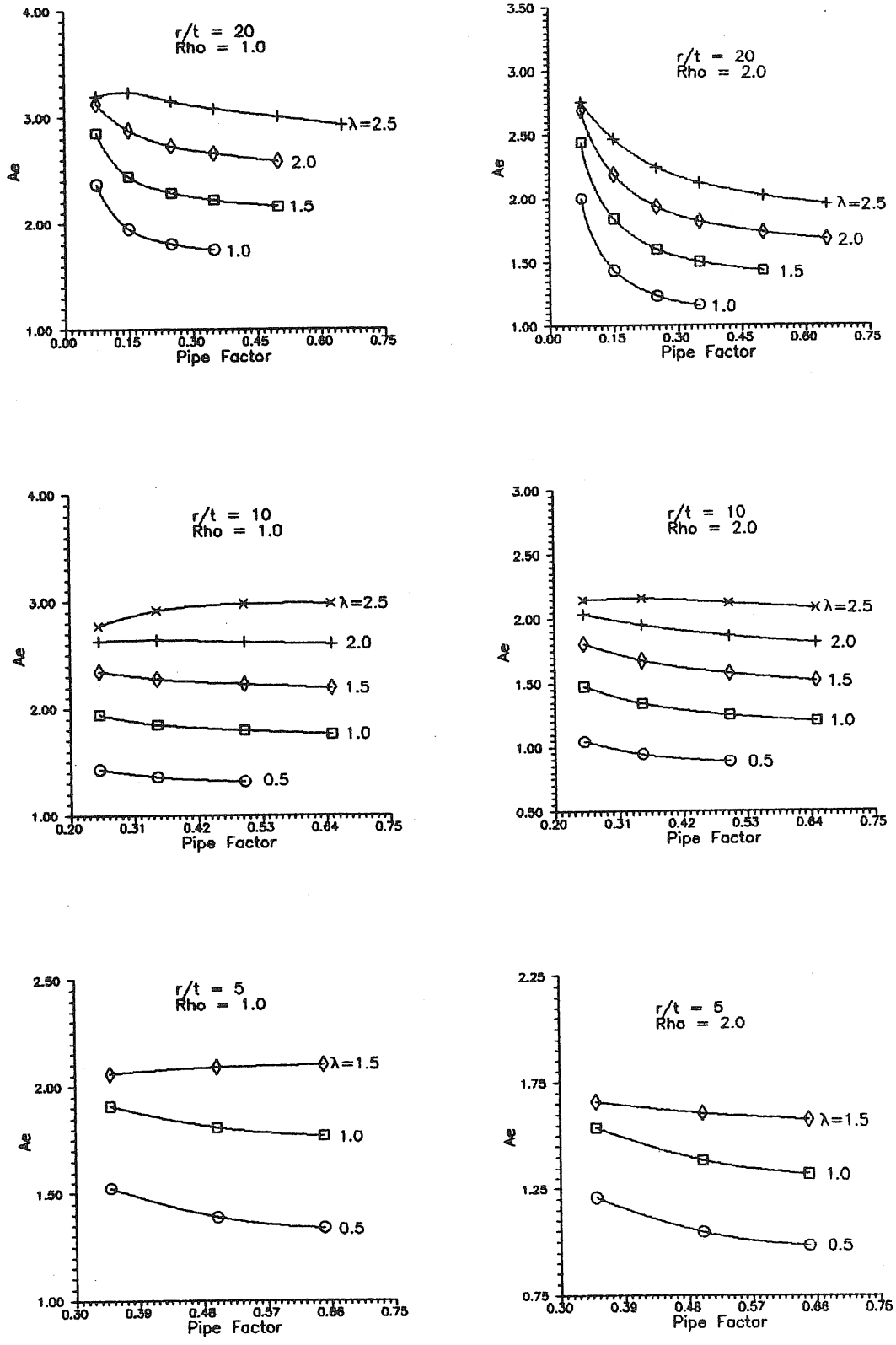

Fig. 12b. Variation of A_e with pipe factor (h), r/t and crack length (λ) for a longitudinally cracked elbow ($\rho = 1, 2$).

Table 2. Derived coefficients (C_n) and exponents (p_n) for a circumferential crack

ρ	∞	2	1	0·5	0
C_1	−3·4628	−1·3918	−0·2061	−0·4564	0·2510
C_2	4·446	1·3331	−0·2688	−0·0928	0·2245
C_3	−52·429	−45·488	1·0052	53·608	−7·8911
C_4	52·445	41·612	3·1153	193·82	5·2822
C_5	−2·2524	−0·8677	−0·1474	0·1784	0·0773
C_6	1·1102	0·8342	0·4177	0·2258	0·0599
C_7	0·8634	2·5685	1·8792	2·2646	0·5119
C_8	1·7283	2·1310	1·3741	2·0149	3·0222
p_1	0·1366	0·1574	3·4968	5·4819	−0·0405
p_2	−0·1848	−0·2604	−0·3772	−0·4787	0·1994
p_3	2·6137	4·0769	2·6686	10·248	1·3462
p_4	0·1216	0·1370	0·3705	−0·1983	0·0166
p_5	0·0695	0·0044	−0·116	0·0076	−0·3614
p_6	0·4587	1·1139	1·1723	1·1981	1·2298
p_7	−0·5119	−0·2564	−0·2955	−0·2474	−0·3662

Table 3. Derived coefficients (C_n) and exponents (p_n) for a longitudinal crack

ρ	2	1	0·5	0
C_1	−1·8531	0·6716	0·509	0·5904
C_2	0·0050	0·1932	0·584	0·7452
C_3	1·3618	0·6006	0·3375	−0·5249
C_4	1·1382	0·4195	0·5764	0·5366
C_5	−1·8117	−0·6402	−0·8963	0·1675
C_6	0·0660	−0·0005	0·5076	0·1727
C_7	2·4713	0·1909	−0·2026	0·3639
C_8	0·2726	0·3577	0·74	0·6092
P_1	−1·2866	−0·7353	−0·0426	0·0974
P_2	−0·016	−0·0239	0·1096	0·027
P_3	0·4025	0·1440	0·2889	3·986
P_4	−1·2083	−1·9603	−0·2266	0·0539
P_5	−0·5277	0·1927	0·1229	0·0257
P_6	−0·2421	0·7982	0·9113	0·9089
P_7	0·3353	−0·2501	−0·2676	−0·2039

between the results obtained in the above two cases.

(c) In the case of the analysis of a non-weakened elbow under internal pressure, the hoop and longitudinal stress variations at the elbow mid-plane have excellent agreement with those given in Ref. 8 (Fig. 7).

(d) From the parametric study of an elbow with circumfential crack at the extrados, the following points may be noted:

(i) A small circumferential throughwall crack at the extrados of the elbow does not open up under closing bending moment.
(ii) The A_e increases with the crack angle (θ_c) for all cases.
(iii) For higher values of pipe factors (h), A_e seems to be independent of h (Fig. 10).

(e) From the parametric study of an elbow with a longitudinal crack at the crown, the following points may be noted:

(i) A longitudinal throughwall crack at the elbow crown does not open fully under pure bending moment.
(ii) The value of A_e increases with crack length (λ).
(iii) In this case also the values of A_e at higher pipe factors are almost independent of h (Fig. 12).

(f) The closed-form expression derived in this work is found to be capable of calculating the stress intensity factor of an elbow with circumferential and longitudinal cracks under combined internal pressure and bending moment for the range of different geometrical parameters considered in this analysis.

REFERENCES

1. Report of the United States Nuclear Regulatory Commission Piping Review Committee, *Evaluation of Potential for Pipe Breaks,* NUREG-CR-1061, Vol. 3. USNRC, Washington, DC, 1984.
2. Kumar, V., German, M. D. & Shih, C. F., *An Engineering Approach for Elastic Plastic Fracture Analysis.* EPRI-NP-1931, Electric Power Research Centre, Palo Alto, CA, July 1981.
3. Kumar, V. *et al., Advances in Elastic Plastic Fracture Analysis.* EPRI-NP-3607, Electric Power Research Centre, Palo Alto, CA, Aug. 1984.

4. Atluri, S. N., *Computational Methods in the Mechanics of Fracture,* Elsevier Science Publishers, 1986.
5. Watanabe, T. *et al., J*-integral analysis of plate and shell structures with throughwall cracks using thick shell elements. *Engg. Fracture Mechanics,* **19** (1984) 1005–12.
6. Chattopadhyay, J., Dutta, B. K. & Kushwaha, H. S., Elastoplastic fracture mechanics analysis of elbows using layered shell bending elements. In *Proc. Int. Symp. on Fatigue and Fracture of Steel and Concrete Structures,* ISSF-91, Madras, India, 1991, pp. 79–89.
7. Barsoum, R. S. *et al.,* Analysis of cylindrical shell with cracks using quarter point crack tip elements. *Int. J. Fracture,* **15** (1979) 259–80.
8. M. W. Kellog Co., *Design of Piping System.* John Wiley, 1967.

ELSEVIER

Int. J. Pres. Ves. & Piping **60** (1994) 297–306

0308-0161/94/$07.00

On line fatigue life monitoring methodology for power plant components

N. K. Mukhopadhyay, B. K. Dutta, H. S. Kushwaha, S. C. Mahajan & A. Kakodkar

Reactor Design and Development Group, Bhabha Atomic Research Centre, Bombay 400085, India

(Received 6 November 1993; accepted 18 November 1993)

Fatigue is one of the most important aging effects of power plant components. Information about fatigue helps in assessing structural degradation of the components and so assists in planning in-service inspection and maintenance. It may also support the future life extension programme of a power plant. In the present paper, the development of a methodology for on line fatigue life monitoring using available plant instrumentation is presented. The Green's function technique is used to convert plant data to stress–time data. Using a rainflow cycle counting method, stress–time data are analysed and the fatigue usage factor is computed from the material fatigue curve. Various codes are developed to generate Green's functions, to convert plant data to stress–time data, to find the fatigue usage factor and to display fatigue information. Using the developed codes, information about the fatigue life of various components of a power plant can be updated, stored and displayed interactively by plant operators.

Three different case studies are reported in the present paper. These are the fatigue analyses of a thick pipe, of a nozzle connected to a pressure vessel and of a reducer connecting a heat exchanger to its piping system.

1 INTRODUCTION

The degradation effect of power plant components is an important consideration for the safety of the plant. Among the various such aging effects, fatigue is one of the most important. This affects plant life especially when a plant approaches the end of its design life. Major factors affecting the fatigue life of a power plant components are the fluctuation of temperature, pressure and flow rate. Information about accumulation of fatigue helps in assessing structural degradation of the components. This assists one to define the in-service inspection and maintenance schedule and may also support a future life extension programme of a power plant based on the actual observation.

The effects of fatigue are estimated and restricted during the design as per the rules given in the ASME boiler and pressure vessel code. End-of-life fatigue usage factors are determined in accordance with these rules. These are calculated assuming a set of conservative design transients to ensure that plant components do not exceed a fatigue usage factor of unity throughout their design life. Many actual plant operating cycles, however, are quite different from the transients assumed in the design. Plant operation is conservatively restricted by the design transients in most of the cases. However there is currently no practical means by which one can take the credit for this implicit margin to extend the useful life of plant components. This can only be achieved by implementing a methodology to monitor and record continuously the actual loading conditions seen by a component during its operation. Subsequent sections show the development of such a methodology.

2 ON LINE FATIGUE LIFE MONITORING METHODOLOGY

It is neither possible nor necessary to monitor the fatigue life of all the components of a power

plant. Fatigue life depends on the magnitude of the stress range and the number of cycles experienced by a component which in turn depend on the process transients seen by that component. A number of critical components which experience the maximum fluctuation of fluid parameters are to be selected for fatigue life monitoring. The plant parameters are measured on line and the fatigue usage factor is continuously updated for the selected components.

A transfer function approach is used to convert plant data to stress versus time data. The stresses are divided into two parts: (i) thermal stresses and stresses due to internal pressure, (ii) external loads including piping loads. Thermal stresses are calculated by a time integration of plant thermal hydraulic parameters through the use of a predetermined set of Green's functions. Stresses due to internal pressure and external loading are superimposed to obtain peak stress versus time history. The peak stress versus time history data developed in this manner are generally irregular in nature. This stress versus time history is to be converted into stress versus frequency spectra to compute the fatigue usage factor.

A 'rainflow cycle counting' method is used to analyse this irregular loading history. The number of cycles experienced by the component is counted and the fatigue usage factor is computed from material fatigue data. This information is to be continuously updated at the monitored highly stressed locations.

Several components of a fossil power plant and a fast breeder nuclear reactor operate at such an elevated temperature that creep behaviour and crack growth due to fatigue–creep interaction are also to be considered in a damage assessment model. On line fatigue monitoring methodology can also be extended to monitor the aging effects due to creep and crack growth owing to the fatigue–creep interaction. Creep damage is estimated from stress-time history using material creep data. The independent damage due to fatigue and creep is considered separately, summed and compared against the limit of damage index which the material can withstand. The accumulated crack growth is estimated by computing both the effects of fatigue and creep separately and then by adding them together. Fatigue crack growth rates are calculated using a linear elastic fracture mechanics technique. Creep crack growth rates are calculated using a time dependent C_t approach.[1] The different steps in on line age monitoring methodology are shown in Fig. 1.

3 GREEN'S FUNCTION TECHNIQUE

The Green's function technique provides a very powerful tool in on line fatigue life monitoring. This technique is used to convert plant data to peak stress–time data as the computation time is much less than the time taken by the finite element method. Closed form solutions of Green's function for certain well defined geometries are presented by Carslaw and Jaeger[2] and Boley and Weiner.[3] However, closed form solutions of Green's function are difficult to derive for the complex geometries generally used in power plants. Hence, for such complex geometries, Green's functions are derived using a finite element method for the unit change of the associated parameter.[4]

3.1 Development of a code for derivation of Green's functions

A computer code GREFIN (GREen's function evaluation by FINite element) has been developed. It has two modules, WELTEM[5] and VENUS.[6] The first module is capable of computing the Green's functions for temperature by a finite element techique for 2-D plane stress, plane strain and axisymmetric geometries. This is capable of considering surface heat transfer through forced or natural convection, volumetric heat generation and isothermal boundary conditions. Depending upon the user's choice, it can consider different types of transient solution algorithms, such as forward difference, backward difference, Galerkin, Crank Nicholson, etc. The second module of the code is a 2-D finite element code to solve plane stress–strain and axisymmetric structures. This module is capable of considering different types of loads such as pressure, concentrated load, gravity load, thermal load, etc. The elements available are four to eight noded isoparametric elements. This module is modified to generate Green's functions for stress by making it compatible with the first module.

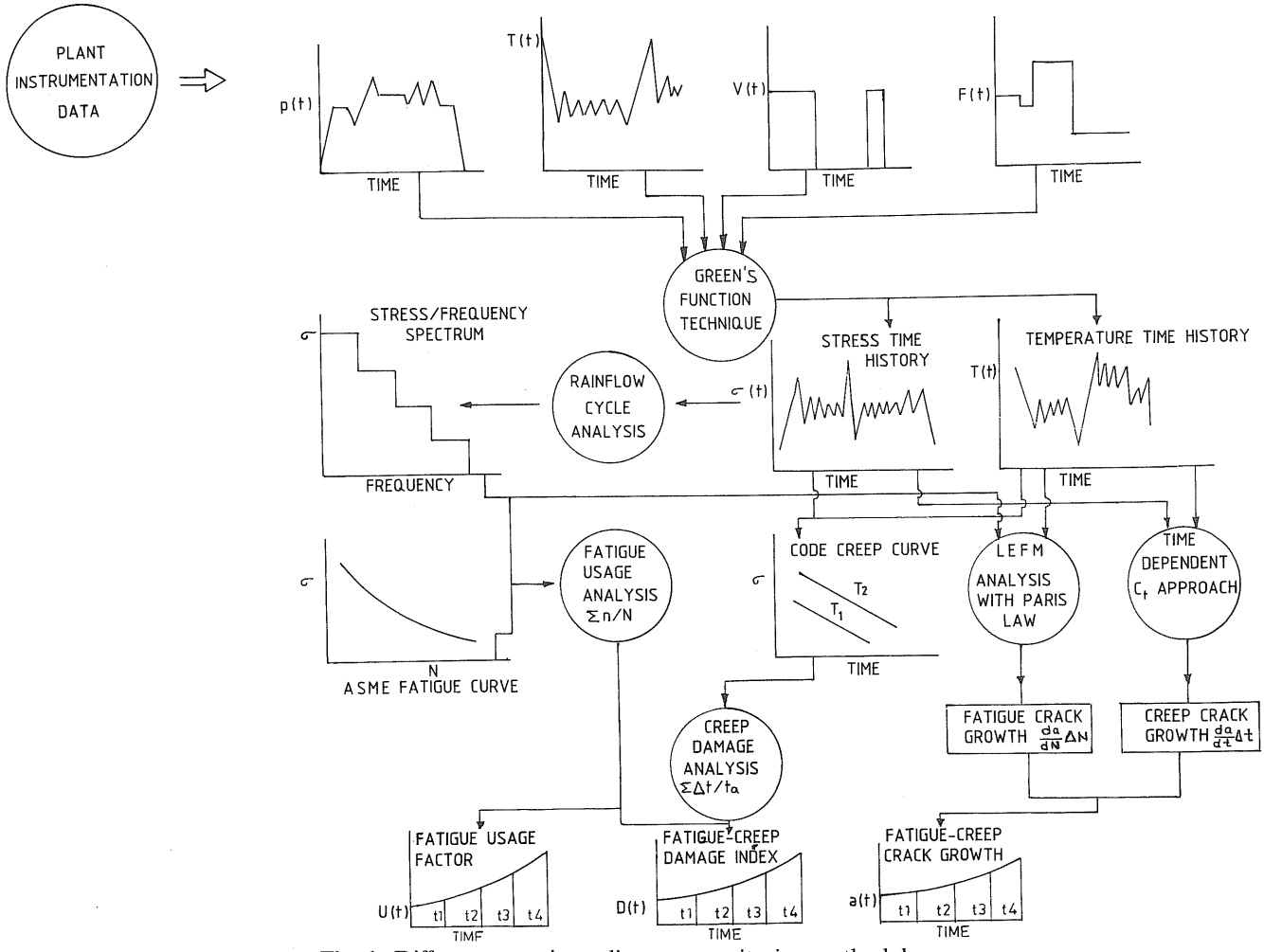

Fig. 1. Different steps in on line age monitoring methodology.

3.2 Development of a code to convert plant data to stress–time history using a Green's function technique

The Green's function technique converts plant transients into temperature–stress responses at a point in the component experiencing the transients. Generally the power plant components are subjected to multiple site (places where fluid parameters are varying) loading. A multiple site (m) problem is decomposed into two single site problems. Each single site problem is solved independently and then superimposed to compute the total effect.

For a multiple site (m) loading problem with the thermal system in a steady state condition with temperature $T_o(x_i)$, stresses $\sigma_0(x_i)$ and fluid temperatures ϕ_0^n (where $n = 1, m$), and subjected to fluid temperature disturbances $\Delta\phi^n(t)$ (where $n = 1, m$), the fluid temperature and stress of the structure can be expressed by the following equations:

$$T(x_i, t) = T_o(x_i) + \sum \Delta T^n(x_i, t) \tag{1}$$

$$\sigma(x_i, t) = \sigma_0(x_i) + \sum \Delta\sigma^n(x_i, t) \tag{2}$$

Here ΔT^n and $\Delta\sigma^n$ are temperature and stress distributions of the nth single site problem respectively, x_i represents the coordinates and the t is time.

A formulation for computing temperature–stress responses using a single site superimposed Green's function technique has been developed by Chen and Kuo.[7] The temperature and stress responses are expressed by the following equations:

$$T(x_i, t) = T_o(x_i) + \sum \left[\overline{G_T^n}(x_i)\, \Delta\phi^n(t) + \int_{t-t_d}^{t} G_T^{n'}(x_i, t-\tau)\, \mathrm{d}\Delta\phi^n(\tau) \right] \tag{3}$$

$$\sigma(x_i, t) = \sigma_0(x_i) + \sum \left[\overline{G_\sigma^n}(x_i)\, \Delta\phi^n(t) + \int_{t-t_d}^{t} G_\sigma^{n'}(x_i, t-\tau)\, \mathrm{d}\Delta\phi^n(\tau) \right] \tag{4}$$

where

$$G^{n'}_{T}(x_i, t) = G^{n}_{T}(x_i, t) - \overline{G^{n}_{T}}(x_i) \quad (5)$$

$$G^{n'}_{\sigma}(x_i, t) = G^{n}_{\sigma}(x_i, t) - \overline{G^{n}_{\sigma}}(x_i) \quad (6)$$

Here $G^{n}_{T}(x_i, t)$ and $G^{n}_{\sigma}(x_i, t)$ are the temperature and stress Green's functions of the nth single site problem. $\overline{G_T}(x_i)$ and $\overline{G_\sigma}(x_i)$ are steady state values of the temperature and stress Green's functions and t_d denotes the decay time.

Using eqns (3) and (4) a post processor has been developed. This post processor SREGRE (Structural REsponse by GREen's functions) computes the total temperature and stress responses taking into consideration the actual change in fluid temperature and flow histories. Simpson's one-third integration rule has been adopted to compute the transient effect. This post processor is capable of handling very long fluid parameter variation histories. Very often the entire fluid parameter history cannot be read into the computer because of limitation in computer memory. The present post processor computes the temperature–stress responses while reading the input data. This makes even a Personal Computer (PC) capable of analysing power plant data for several years.

4 RAINFLOW CYCLE COUNTING METHOD

The rainflow cycle counting method has been proved to be superior to other cycle counting methods for analysing an irregular stress history. In this method the cycle is counted such that small stress excursions are considered as temporary interruptions of larger stress excursions.[8] It matches the highest peak and deepest valley, then the next largest and smallest together, etc., until all peaks and valleys are paired.

4.1 Algorithm of rainflow cycle counting method

Due to the great importance of the rainflow cycle counting method many different algorithms have been proposed in the literature.[9–12] The algorithm presented by Socie[9] requires the entire load history to be known before the counting process starts. As a result, it is not suitable for on line data processing since the entire load history is not known until the end of the test. The one-pass rainflow cycle counting algorithm presented by Downing and Socie[11] overcomes this limitation. This can operate in on line data processing. A rainflow cycle counting algorithm suitable for very long stress histories even with a small computer for on line data processing is described by Glinka and Kam.[12]

The fundamental characteristic of the rainflow cycle counting method is its simplicity in the algorithm. It is also compatible with the corresponding stress–strain relation when it is applied to a strain–time history. It is a wave analysing procedure which takes into account the sequential order of peaks and valleys while ignoring the time duration between the successive peaks and valleys. A means of collecting long term data, using microcomputer devices and interpreting the data in a manner useful to the engineer for fatigue analysis is reported in the literature.[13] A hard-wired logic for the rainflow cycle counting algorithm is described and simulated by Anzai and Endo.[14]

4.2 Development of code to compute the fatigue usage factor using the rainflow cycle counting method

A post processor FRAIN (Fatigue usage factor by RAINflow counting) has been developed. From the peak and valley stresses, this post processor finds out the number of complete cycles experienced by the component using the rainflow cycle counting method. From the appropriate material fatigue data this code also computes the accumulated fatigue usage factor. This post processor is capable of performing rainflow counting without prior knowledge of the whole stress history. Very often the entire stress history which is to be analysed cannot be read at once because of the limitation of the computer memory. Here, the stress history can be read and analysed block by block by computer without reading the whole history at once. This enables personal computers to analyse very long stress histories.

5 DEVELOPMENT OF GRAPHICS CODE

Information on fatigue degradation is to be continuously recorded and updated from the plant transients. In a power plant this is done by an operator. A graphics code IGOLFM (Interactive Graphics On Line Fatigue Monitoring) has been developed to make the methodology user friendly. This code is written in Turbo 'C' and this enables the user to interface among the earlier developed codes. The whole methodology is made menu driven and fatigue analysis can be done componentwise according to the operator's choice. Using this code the monitored transients can be analysed and information can be updated, stored and displayed when necessary. An efficient file management has been done to optimise the number of files. On line transients for a number of components of a power plant can be simultaneously processed, recorded and stored using a personal computer 386.

6 CASE STUDIES

6.1 Analysis of a thick pipe subjected to multiple site loading

The first case study deals with the analysis of a thick pipe in a power plant having temperature and flow variation on both inside and outside surfaces. Figure 2(a) shows the geometrical dimensions, material properties and heat transfer coefficients used in this problem. The fluid temperature variations at the inner and outer surfaces are assumed to vary in a manner as shown in Fig. 2(b). A finite element discretisation has been done using axisymmetric eight noded elements. The flow rate is assumed to vary between a range such that h_i (inside heat transfer coefficient) varies between 141·85 and 1134·8 W/m^2 K (25 and 200 Btu/ft^2 h °F). Using the developed code GREFIN the temperature and stress Green's functions were computed for both inside and outside temperature variations with two different h_i values. These temperature and stress Green's functions are shown in Figs 2(c) and 2(d) respectively.

A single site problem was solved considering only the inside fluid temperature variation with a constant h_i value of 1134·8 W/m^2 K (200 Btu/ft^2 h °F). The temperature and stress responses at the inner surface were computed using the corresponding temperature and stress Green's functions. These results are shown in Fig. 3 as curve 1. For the next case, the fluid temperatures at the inner and outer surfaces were assumed to vary simultaneously. This multiple site loading

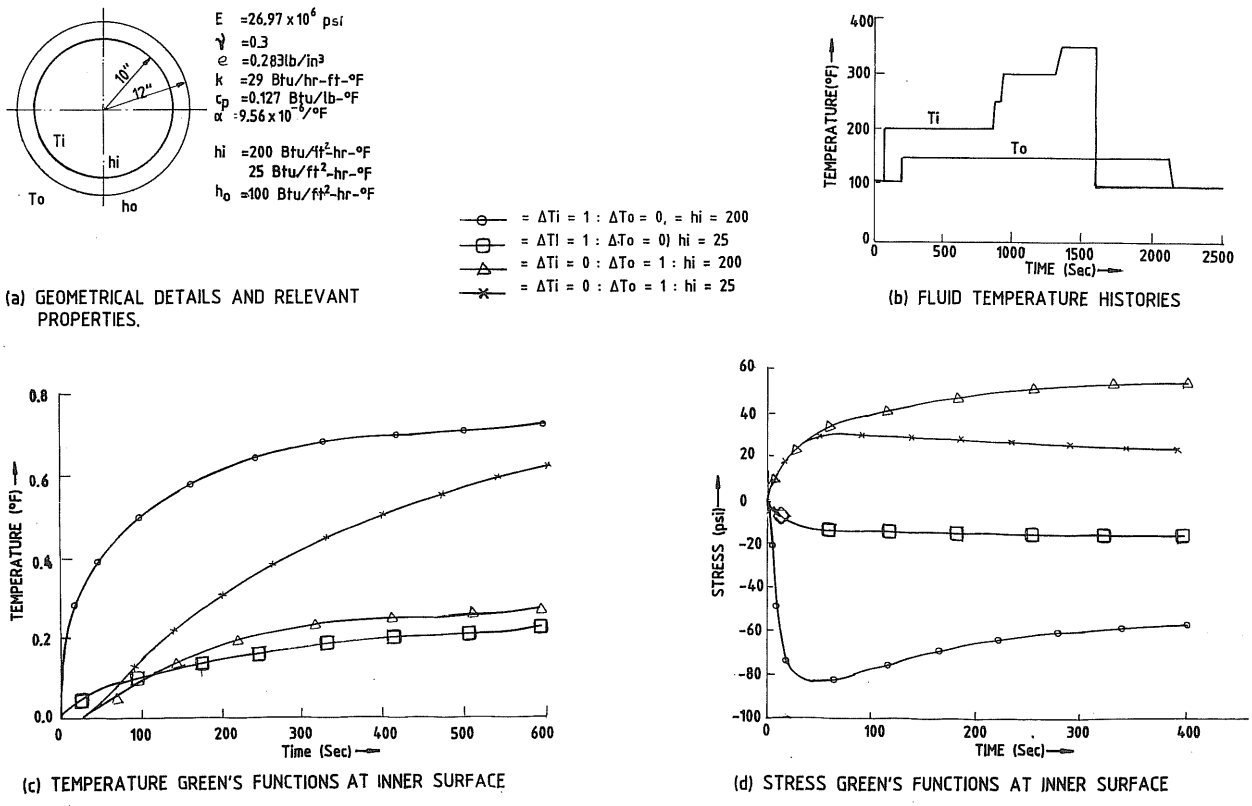

(a) GEOMETRICAL DETAILS AND RELEVANT PROPERTIES.

(b) FLUID TEMPERATURE HISTORIES

(c) TEMPERATURE GREEN'S FUNCTIONS AT INNER SURFACE

(d) STRESS GREEN'S FUNCTIONS AT INNER SURFACE

Fig. 2. Problem definition and Green's functions for case study-1.

problem was decomposed into two single site loading problems and the response for each loading was computed and superimposed to obtain the actual response. The temperature and stress responses are computed and shown in Fig. 3 as curve 2. A detailed finite element calculation was also performed for both cases. These results are also plotted in Fig. 3.

The third case in this example considers variation of fluid temperature and h_i simultaneously. A typical variation is shown in Fig. 4(a). A new set of temperature and stress Green's functions were computed for a change in h_i from 141·85 to 1134·8 W/m^2 K (25 to 200 Btu/ft^2 h °F) after a time of 800 s.

These are shown in Fig. 4(b). The temperature and stress responses using Green's functions are shown in Fig. 4(c). To verify the results finite element solutions are also obtained, which are shown in Fig. 4(c).

6.2 Analysis of a nozzle connected to a spherical head of a pressure vessle

This case study deals with a nozzle connected to a spherical head of a cylindrical pressure vessel. It is exposed to fluid temperature fluctuations. Figure 5(a) shows the geometrical dimensions, material properties and heat transfer coefficients of the problem. A typical fluid temperature variation is assumed on the vessel and nozzle surfaces as shown in Fig. 5(b). A finite element discretisation has been done using axisymmetric four noded elements to generate Green's functions. This discretisation is shown in Fig. 5(c). Temperature and stress Green's functions due to a unit rise in temperature of the nozzle side fluid and vessel side fluid were computed separately. The temperature Green's function was computed for point 'A' (Fig. 5(a)), whereas the stress Green's function was computed for the centre of the element surrounding point 'A'. These Green's functions are shown in Fig. 6(a). These Green's functions were then used to compute temperature and stress responses for the given fluid temperature transients (Fig. 5b)). These are shown in Fig. 6(b).

6.3 Analysis of a reducer joining a heat exchanger to an outlet pipe of a nuclear plant

A heat exchanger connected to its piping system through a reducer used in a nuclear plant is studied. The temperature of the fluid is continuously monitored as it comes out of the heat exchanger. This temperature was observed

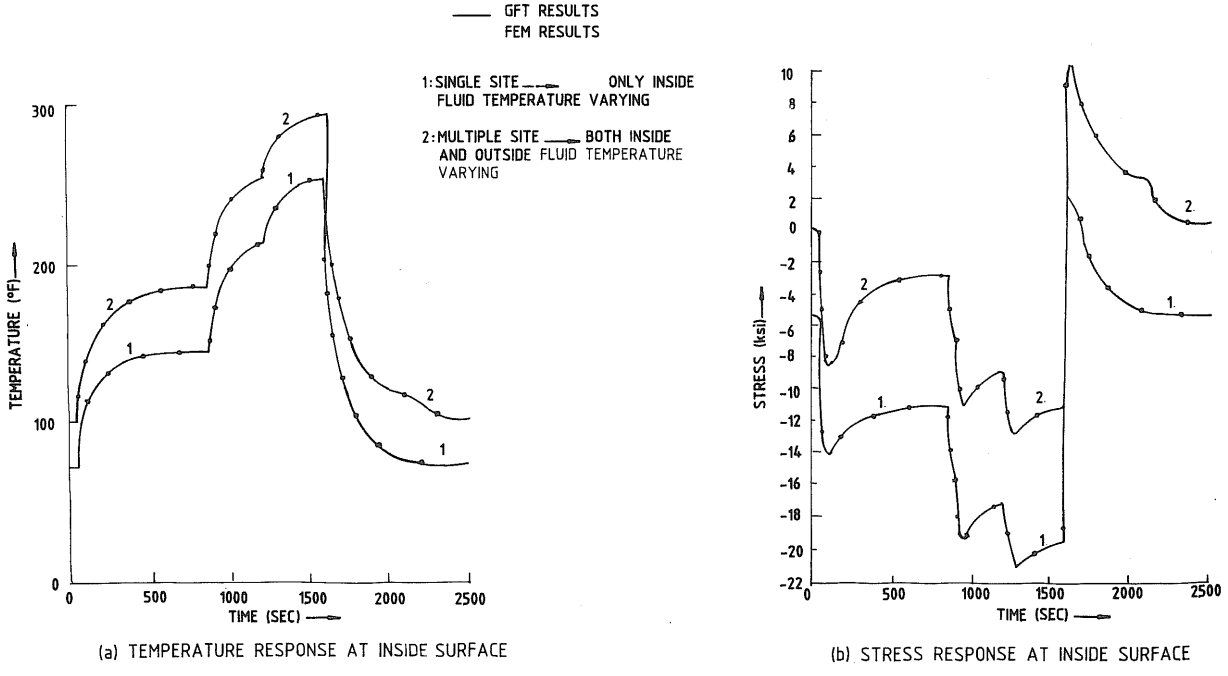

(a) TEMPERATURE RESPONSE AT INSIDE SURFACE

(b) STRESS RESPONSE AT INSIDE SURFACE

Fig. 3. Temperature and stress responses of case study-1 due to fluid temperature fluctuations.

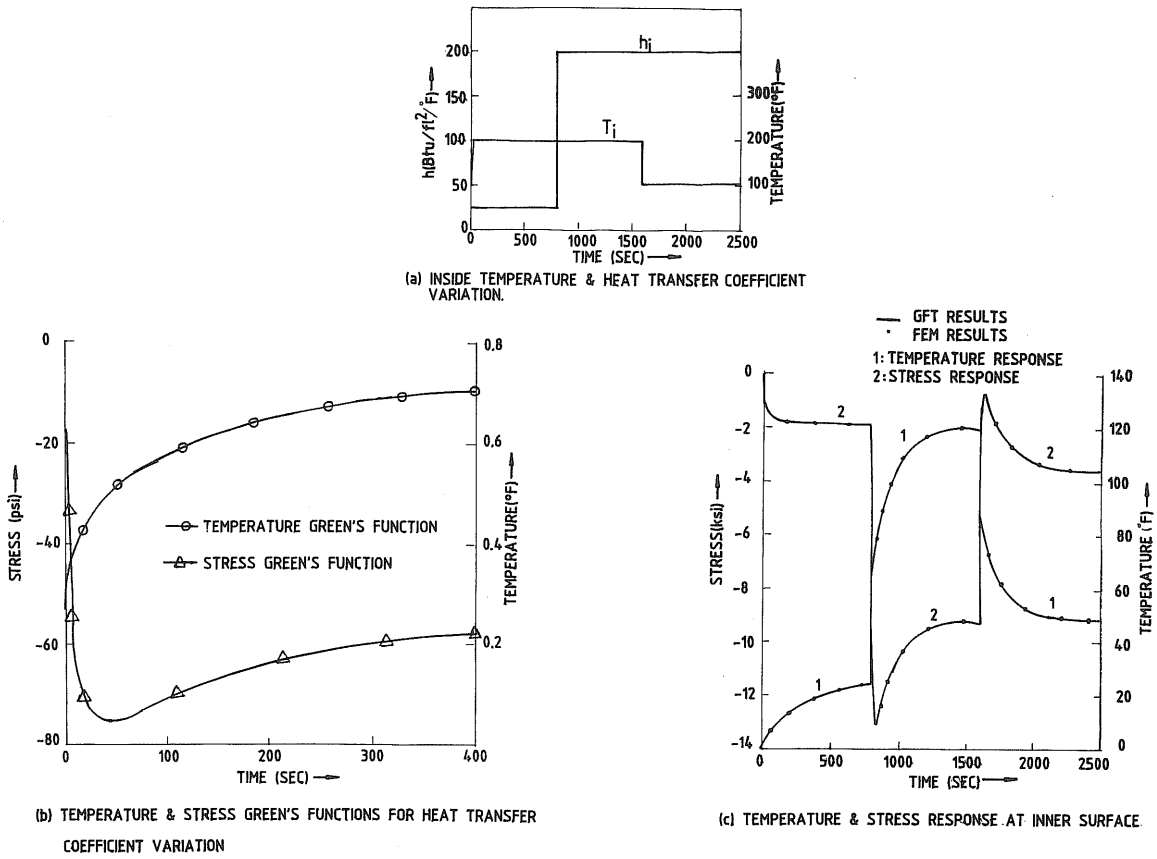

Fig. 4. Analysis of effects of heat transfer coefficient variation in case study-1 and comparison of results with FEM.

to be varying with time. Stresses were found to be moderately high in the reducer due to discontinuity in the geometry. The geometrical details, material properties and fluid heat transfer coefficient are shown in Fig. 7(a). The reducer is insulated at its outer surface, hence the problem is a single site thermal loading problem. The fluid temperature is recorded by gas thermometer; nearly 27 days fluid temperature data have been studied here. The fluid temperature variation is shown in Fig. 7(b).

A finite element discretisation has been done using axisymmetric four noded elements. The stress Green's function was derived for the point 'A' which is found to be the critical location. This stress Green's function is shown in Fig. 7(c). The stress response at 'A' due to the fluid temperature fluctuations was determined. The peak and valley stresses are shown in Fig. 7(d). The stress range and mean stress of the cycles experienced by the component were determined by a rainflow cycle counting method. For each cycle the fatigue usage factor was computed from the material fatigue data[15] and these were added to compute the accumulated fatigue usage factors for all cycles counted. The cycles counted as derived by the rainflow cycle method are grouped into several bands of stress ranges and are shown in Fig. 7(e).

7 CONCLUSIONS

The following conclusions are drawn from the above analysis:

—Development of a methodology has been shown which can be efficiently used for on line monitoring of the fatigue usage factor of different components of a power plant.

—The fast computation of stress transients is required for on line monitoring methodology. This can be achieved by using the Green's function techique.

—The Green's function technique is found to be as accurate as any other numerical method such as the finite element technique (Case study 1).

—The excellent agreement of the results computed using Green's function with the results of finite element analysis prove that the multiple site loading problem can be very

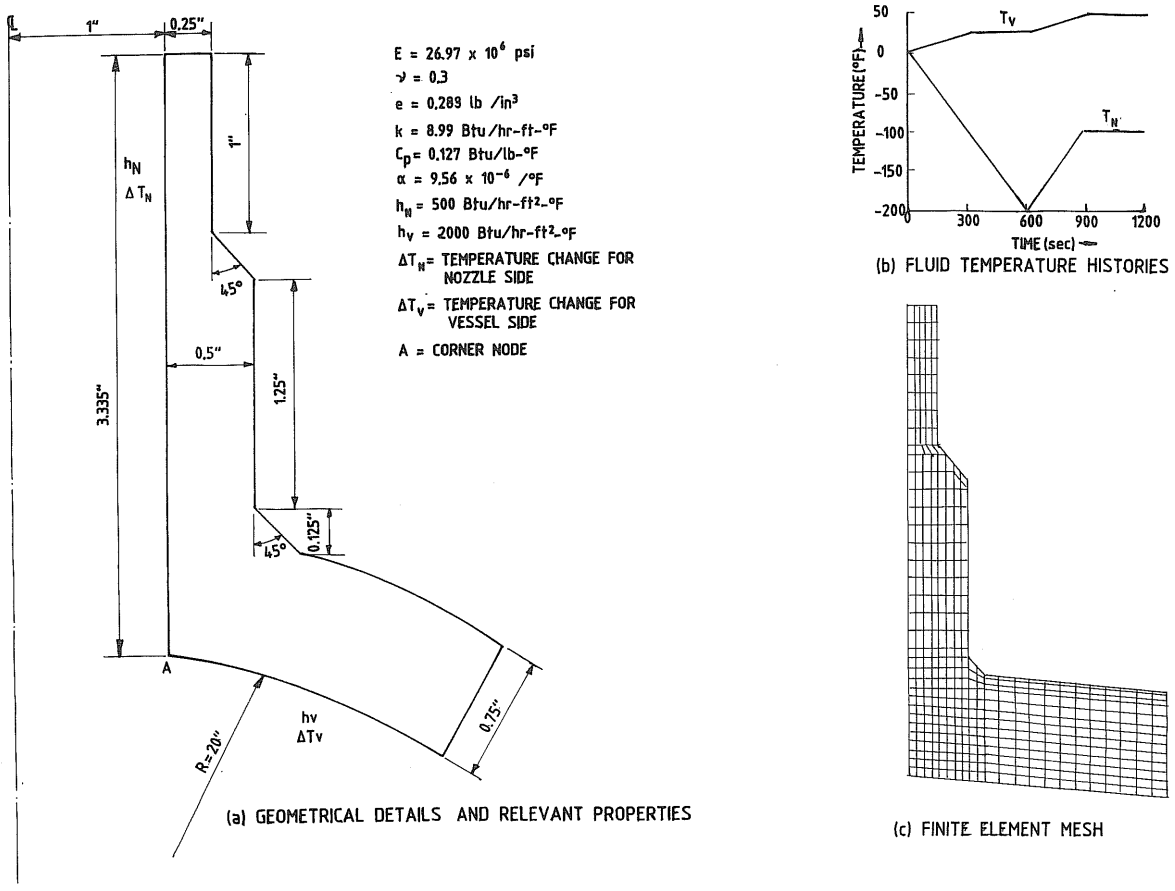

Fig. 5. Problem definition and finite element mesh for Green's function evaluation for case study-2.

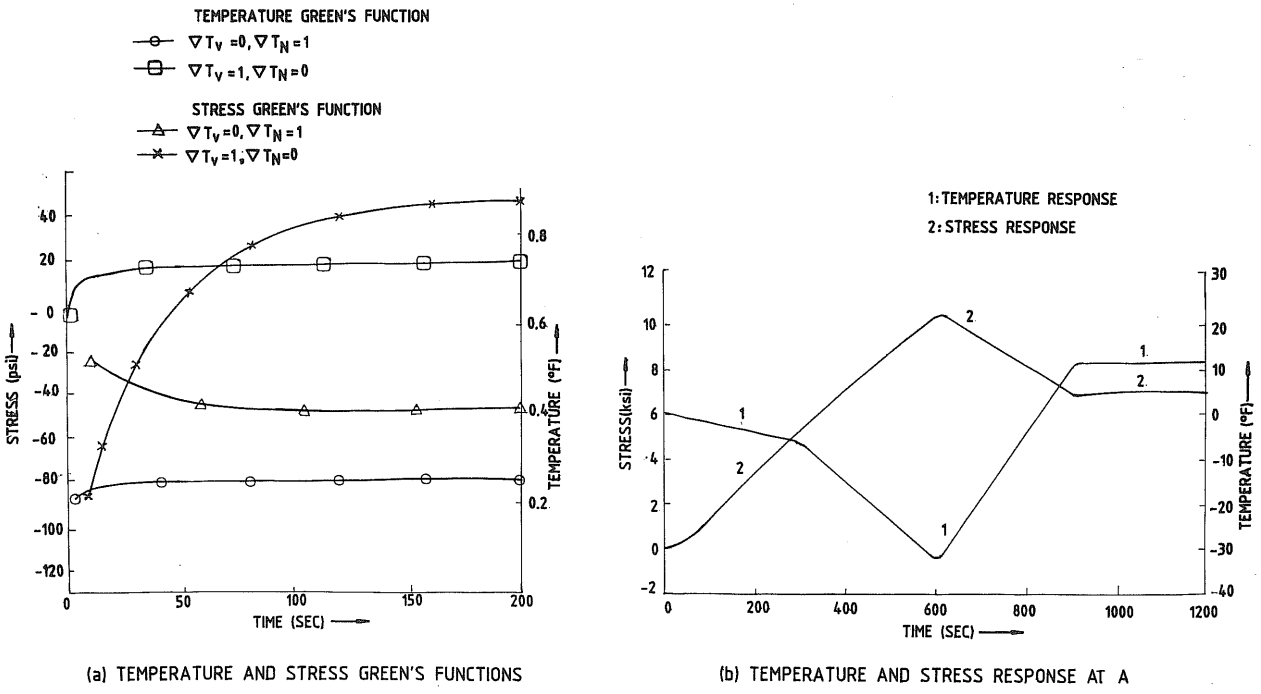

Fig. 6. Green's functions, temperature and stress response for case study-2.

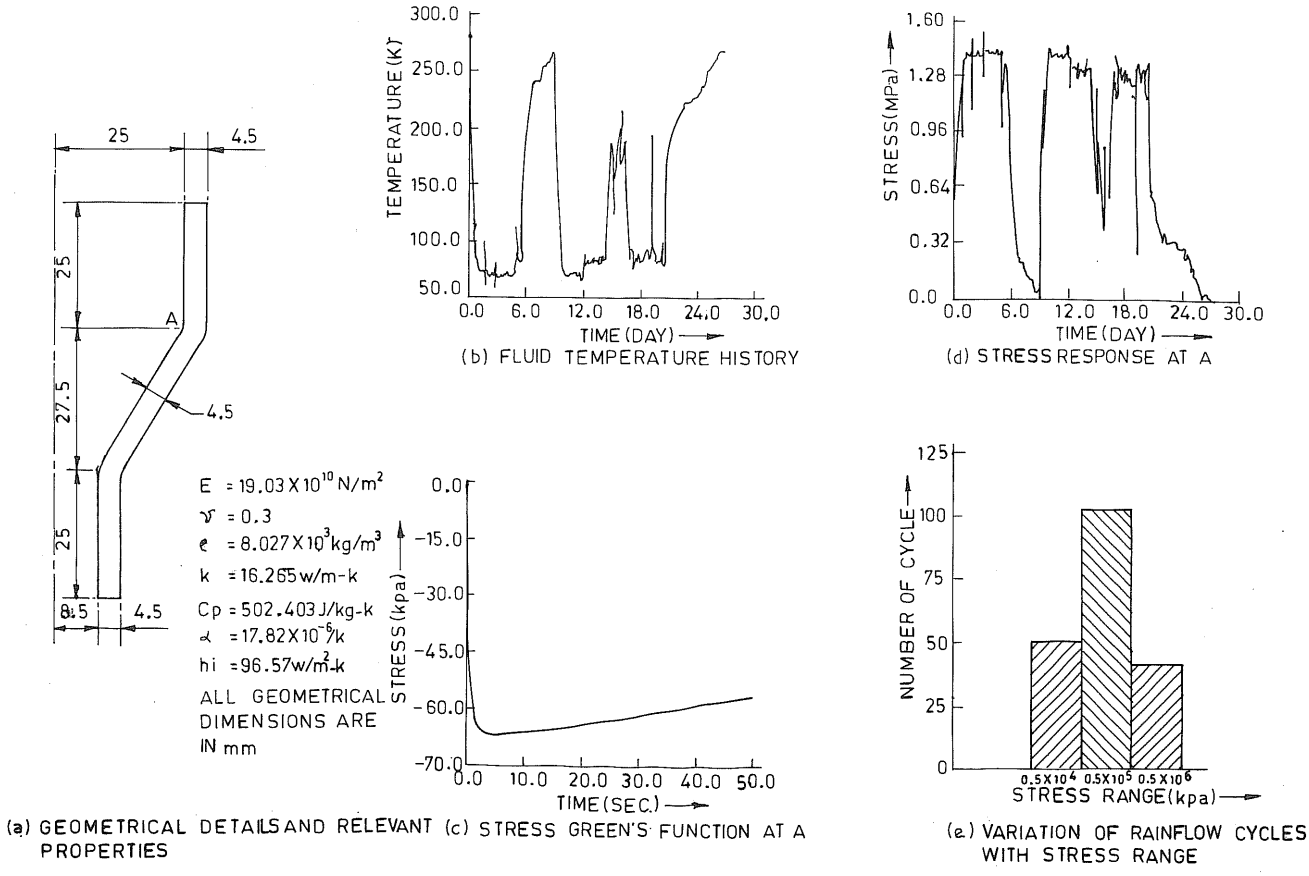

Fig. 7. Fatigue cycle evaluation for reducer of a heat exchanger subjected to fluid temperature variation.

efficiently solved using a single site superimposed Green's function technique.

—However the Green's function technique can not be used in the cases where nonlinearities are involved such as material properties changing with temperature, yielding of material at geometrical discontinuity, rapid variation of heat transfer coefficients. However, through the present study, it is found that the variation of heat transfer coefficients can be considered in the case of discrete variations. This is done by generating Green's functions for different values of heat transfer coefficient separately.

—Development of the present methodology has proved that the Green's function technique and rainflow cycle counting method can be efficiently used for on line monitoring of fatigue usage factors from process transients.

—On line transients of a large number of components of a power plant can be processed, stored and displayed when necessary as the computation time taken in this methodology is low.

—This fatigue monitoring methodology can be further extended to provide information about the creep and crack growth rate of the components operating at an elevated temperature.

REFERENCES

1. Saxena, A., Sherlock, T. P. & Viswanathan, R., Evaluation of remaining life of high temperature headers: a case history. *Proceedings of EPRI workshop on life extension and assessment of fossil plant,* 1988.
2. Carslaw, H. S. & Jaeger, J. C., *Conduction of Heat in Solids,* 1st edn. Clarendon Press, Oxford, 1947.
3. Boley, B. A. & Weiner, J. H., *Theory of Thermal Stresses,* 1st edn. John Wiley, New York, 1960.
4. Bimont, G. & Aufort, P., Fatigue monitoring in nuclear power plant. *Structural Mechanics in Reactor Technology,* **9** (1987) 133–40.
5. Dutta, B. K., Kushwaha, H. S. & Kakodkar, A., *Computer Program WELTEM* (Analysis of two dimensional heat transfer problems by finite element technique) *Theory and User's Manual.* BARC/I-671, 1981.

6. Dutta, B. K., A 2-D thermo-mechanical finite element model for residual stress determination during welding and annealing. M.Tech thesis to Mechanical Engineering Department, IIT, Kanpur, 1983.
7. Chen, K. L. & Kuo, A. Y., Green's function technique for structures subjected to multiple site thermal loading. *Structural Mechanics in Reactor Technology,* **11D** (1991) 353–8.
8. Deardorff, A. F. & Kuo, A. Y., Advancements in transient thermal stress analysis for application in reactor transient fatigue monitoring, Structural Integrity Associates, San Jose, CA. *Structural Mechanics in Reactor Technology,* **10** (1989).
9. Socie, D. F., Fatigue life prediction using local stress strain concepts. *Experimental Mechanics,* **17** (1977) 50–6.
10. Rychlik, I., A new definition of the rainflow cycle counting method. *International Journal of Fatigue,* **9** (1987) 119–121.
11. Downing, S. D. & Socie, D. F., Simple rainflow counting algorithm. *International Journal of Fatigue,* **4** (1982) 31–40.
12. Glinka, G. & Kam, J. C. P., Rainflow counting algorithm for very long stress histories. *International Journal of Fatigue,* **9** (1987) 223–8.
13. Socie, D. F., Shifflet, G. & Berns, H., A field recording system with applications to fatigue analysis. *International Journal of Fatigue,* **1** (1979) 103–11.
14. Anzai, H. & Endo, T., On site indication of fatigue damage under complex loading. *International Journal of Fatigue,* **1** (1979) 49–57.
15. *ASME Boiler and Pressure Vessel Code,* Section III, Division I, Appendix, 1986.